



Partial physicochemical properties and relative stability of polyhydroxylated dibenzofurans: Theoretical and experimental study

Jia-Qi Shi^a, Jing Qiu^a, Li Sun^a, Meng Wang^a, Fu-Yang Wang^b, Zun-Yao Wang^{a,*}

^a State Key Laboratory of Pollution Control and Resources Reuse, School of the Environment, Nanjing University, Nanjing 210046, PR China

^b School of the Jinling, Nanjing University, Nanjing 210089, PR China

ARTICLE INFO

Article history:

Available online 12 June 2012

Keywords:

Polyhydroxylated dibenzofuran
Hydrogen bond
Partition and ionization
Relation between properties and substitution
Relative stability

ABSTRACT

Polyhydroxylated dibenzofuran (PHODF) is an important degradation product of polychlorinated dibenzofuran (PCDF). Four types of hydrogen bonds (the one between a hydroxyl and the oxygen atom in the matrix, between hydroxyls at *ortho* positions, between the oxygen atom of hydroxyl at position 1 and the hydrogen atom of the matrix at position 9, and between hydroxyls at positions 1 and 9) exist in PHODFs. The energies of the hydrogen bonds were ascertained by comparing the two configurational isomers as approximately 8–11 kJ mol⁻¹, 16–21 kJ mol⁻¹, 5–8 kJ mol⁻¹ and 23–25 kJ mol⁻¹, respectively. An experiment was designed to verify the bond energies, and the entrance geometry on main paths was studied by AIM 2000 program. The most stable in each group of configurational isomers was ascertained on the basis of evaluating the effect of hydrogen bonds. Their thermodynamic properties (standard state entropy S° , standard enthalpy $\Delta_f H^\circ$ and standard Gibbs energy of formation $\Delta_f G^\circ$) were calculated from the combination of density functional theory (DFT) at B3LYP/6-311G** level and isodesmic reactions. Octanol/water partition coefficients ($\log K_{ow}$) were calculated on line with molinspiration methodology based on group contributions. The number and position of hydroxyl substitution (N_{PHOS}) can be a good indicator of these properties for all stable PHODF congeners. The configurations most likely to form are those with a hydrogen bond (Type IV). How intramolecular hydrogen bond influences ionization was also investigated and the first-order ionization constant for each stable conformation was obtained with the self-consistent reaction field (SCRF) method.

© 2012 Elsevier Inc. All rights reserved.

1. Introduction

The persistent organic pollutants (POPs) such as polychlorinated dibenzo-*p*-dioxins (PCDDs) and polychlorinated dibenzofurans (PCDFs), are released into the environment during the combustion of materials such as fossil fuels and hydrocarbons [1]. They have been studied extensively owing to the high toxicity [2,3]. PCDFs have been measured at various sites around the globe [4–7]. It is well documented that PCDFs have adverse biological effects and high toxicities, and consequently are important targets of source reduction. Under atmospheric conditions, PCDFs react with OH[•], NO₃[•], and O₃. But the reaction rates of PCDFs with NO₃[•] and O₃ are so slow that the reaction with OH[•] is the primary pathway. So in the environment, polyhydroxylated dibenzofuran (PHODF) is an important degradation product of PCDF [8]. Manuela Gesell [9] found that in the soil, the biotransformation of the filamentous fungus *Paecilomyces lilacinus* can make the dibenzofuran (DF) hydroxylated. Under atmospheric conditions, the degradation of DF

is initiated by HO[•] addition [8]. In addition, during DF degradation by *Sphingomonas* sp. strain HH69, PHODF is detected as a product [10].

There is little research concerning the environment-related properties of PHODF. This work focuses on the thermodynamic data, hydrophobicity and first-order ionization constant, which are all closely related to the generation, degradation and potential environmental risk of chemicals [11–13]. The structure and carbon atomic numbering of DF are illustrated in Fig. 1.

In PHODFs, hydrogen bonds can form. The hydroxyl orientation will affect the strength of hydrogen bond and the configurational stability. There is little practical method for calculating the intramolecular hydrogen bond energy, so computational approaches are of particular importance. Various computational methods for estimating intramolecular hydrogen bond energy were proposed despite none of them were exact [14–16]. To the best of our knowledge, the most frequently adopted methods are as follows [17]: *cis/trans* analysis, isodesmic reactions, local potential energy density, conformational analysis, and empirical energy-geometry correlations. In this study, molecules were fully optimized with DFT method which has been widely used in various fields [18–21]. And thus thermodynamic properties (standard state entropy S° ,

* Corresponding author. Tel.: +86 25 89680358; fax: +86 25 89680358.

E-mail address: wangzun315cn@163.com (Z.-Y. Wang).

absolute enthalpy H° and Gibbs free energies G°) were obtained. The standard enthalpies of formation ($\Delta_f H^\circ$) and the standard Gibbs energies of formation ($\Delta_f G^\circ$) were also obtained by designing isodesmic reactions. The energy of intramolecular hydrogen bond was obtained by the comparison of $\Delta_f G^\circ$. An experiment was designed to verify the calculation. The octanol/water partition coefficients ($\log K_{ow}$) values of the stable conformers were calculated based on group contribution method. Then correlations of $\log K_{ow}$, $\Delta_f H^\circ$ and $\Delta_f G^\circ$ with the number and position of hydroxyl substitution (N_{PHOS}) were discussed. According to the relative magnitude of their $\Delta_f G^\circ$, the relative stability order of PHODF congeners was theoretically proposed. As ionization is also an important property of chemicals and the focus of many researches [22,23], the influence of hydrogen bond on ionization was also explored and first-order ionization constant (pK_{a1}) of each congener was obtained. It is hoped that this work could contribute to the knowledge of relationship between intramolecular hydrogen bond and environment-related properties about hydroxylated chemicals.

2. Computational and experimental method

In the study, the isomers with one to eight HO– are symbolized as mono-HODF, di-HODF, tri-HODF, tetra-HODF, penta-DF, hexa-HODF, hepta-HODF and octa-HODF, respectively. The name of a molecule depends on the position and orientation of the hydroxyls. The orientation where the hydroxyl faces the oxygen

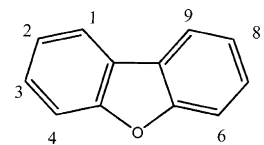
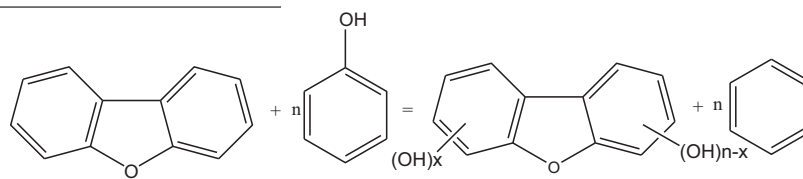


Fig. 1. Molecular structure and atomic number of DF.

positions 1 or 9 is defined as N_1 , the number of HO– at positions 2 or 8 is defined as N_2 , the number of HO– at positions 3 or 7 is defined as N_3 , the number of HO– at positions 4 or 6 is defined as N_4 , and the pair number of HO– at positions 1,9 is defined as $N_{1,9}$. The pair number of *ortho*, *meta* and *para* positions of HO– on one benzene ring is symbolized as N_o , N_m and N_p , respectively. For example, as for OHODF, N_1 – N_4 are all 2, $N_{1,9}$ is 1, and N_o , N_m and N_p are 6, 4, 2, respectively, which are shown in Fig. 2. The parameters mentioned above are defined as a general designation N_{PHOS} [24].

The theoretical calculations on PHODF were performed by DFT method using Gaussian 09 program on 6-311G** basis set. Each molecule was limited as planar during the optimization process. There are no negative frequencies in the calculation result of vibration analysis. All the calculations were scaled by 0.967 so that known systematic errors in calculated frequencies might be eliminated. Thermodynamic parameters, including S° , H° and G° , were obtained directly from Gaussian 09 output files.

The following isodesmic reaction was designed to calculate the $\Delta_f H^\circ$ and $\Delta_f G^\circ$ of PHODF [25].

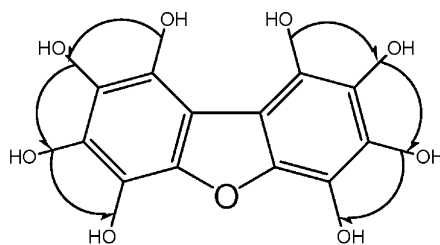


(1)

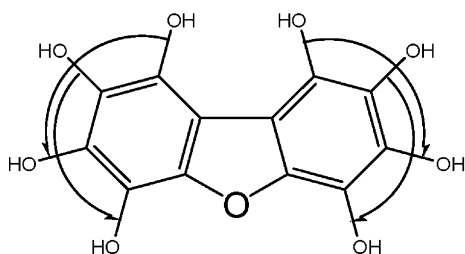
Eqs. (2) and (3) could be obtained.

$$\Delta_f H^\circ = [H^\circ(\text{PHODF}) + nH^\circ(\text{benzene})] - [H^\circ(\text{DF}) + nH^\circ(\text{phenol})] \quad (2)$$

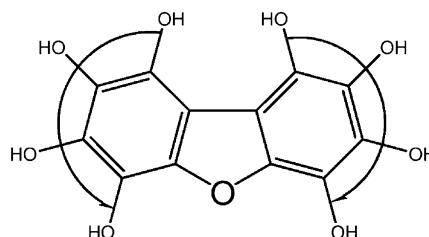
in the matrix was defined as positive, named as 1-, 2-, 3-, 4-, 6-, 7-, 8-, 9-, respectively. Conversely the orientation where the hydroxyl faces away from the oxygen in the matrix as negative, named as 1'-, 2'-, 3'-, 4'-, 6'-, 7'-, 8'-, 9'-, respectively. The number of HO– at



$N_o = 6$



$N_m = 4$



$N_p = 2$

Fig. 2. N_o , N_m , N_p of OHODF.

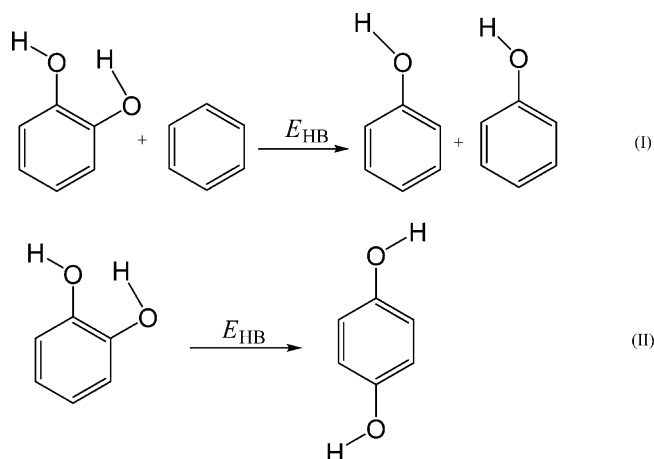


Fig. 3. The two kinds of isodesmic reactions for the determination of E_{HB} .

$$\Delta_f H^\circ = [\Delta_f H^\circ(\text{PHODF}) + n \Delta_f H^\circ(\text{benzene})] - [\Delta_f H^\circ(\text{DF}) + n \Delta_f H^\circ(\text{phenol})] \quad (3)$$

The $\Delta_f H^\circ$ of PHODF can be expressed as Eq. (4):

$$\begin{aligned} \Delta_f H^\circ(\text{PHODFs}) &= H^\circ(\text{PHODFs}) + n H^\circ(\text{benzene}) \\ &\quad - n H^\circ(\text{phenol}) - H^\circ(\text{DF}) - n \Delta_f H^\circ(\text{benzene}) \\ &\quad + n \Delta_f H^\circ(\text{phenol}) + \Delta_f H^\circ(\text{DF}) \end{aligned} \quad (4)$$

Similarly, $\Delta_f G^\circ(\text{PHODFs})$ could be obtained by Eq. (5):

$$\begin{aligned} \Delta_f G^\circ(\text{PHODFs}) &= G^\circ(\text{PHODFs}) + n G^\circ(\text{benzene}) - n G^\circ(\text{phenol}) \\ &\quad - G^\circ(\text{DF}) - n \Delta_f G^\circ(\text{benzene}) + n \Delta_f G^\circ(\text{phenol}) \\ &\quad + \Delta_f G^\circ(\text{DF}) \end{aligned} \quad (5)$$

The experimental values of $\Delta_f H^\circ$ and $\Delta_f G^\circ$ for benzene are 82.9 kJ mol^{-1} and $129.70 \text{ kJ mol}^{-1}$, and those for phenol are $-96.4 \text{ kJ mol}^{-1}$ and $-32.87 \text{ kJ mol}^{-1}$ [26], respectively. The calculated values of H° and G° for benzene at the B3LYP/6-311G** level are $-609649.11 \text{ kJ mol}^{-1}$ and $-609729.07 \text{ kJ mol}^{-1}$, and those for phenol are $-807186.57 \text{ kJ mol}^{-1}$ and $-807279.70 \text{ kJ mol}^{-1}$, respectively. They are also limited to be planer, with the framework group value of D_{6H} for benzene and C_5 for phenol. The experimental values of $\Delta_f H^\circ$ and $\Delta_f G^\circ$ for DF are $47.30 \text{ kJ mol}^{-1}$ and $142.48 \text{ kJ mol}^{-1}$ respectively [27], and the calculated values of H° and G° for DF are $-1410300.22 \text{ kJ mol}^{-1}$ and $-1410411.72 \text{ kJ mol}^{-1}$ at the B3LYP/6-311G** level. The energy of an intramolecular hydrogen bond was obtained from the difference of $\Delta_f G^\circ$ between two isomers [17]. Take catechol as an example, two kinds of isodesmic reactions for the determination of the intramolecular hydrogen bond energy (E_{HB}) are presented in Fig. 3. Based on the isodesmic reaction I, the E_{HB} value in catechol obtained at the B3LYP/6-311G** level is $1.810 \text{ kJ mol}^{-1}$. Clearly, it is much lower than the strength of intramolecular hydrogen bond. The E_{HB} calculated according to the isodesmic reaction II is $10.260 \text{ kJ mol}^{-1}$. It is closer to the actual energy of hydrogen bond. The conjugated system of the hydroxyls in the molecules on both sides of equation II are more similar to each other, more consistent with the requirements of isodesmic reaction. For the reaction I, the conjugated system of the hydroxyl in phenol Π_7^8 is less than the conjugated system Π_8^{10} in catechol. Therefore, the calculated E_{HB} value is smaller, with some error. As the geometry difference and spacial bar were considered in this work during the calculation on the hydrogen bond energy, the results may be thought acceptable.

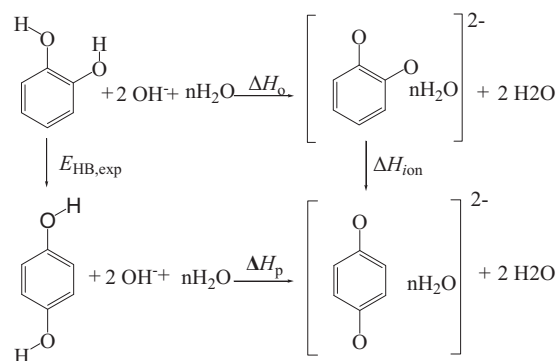


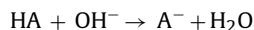
Fig. 4. The schematic diagram for determining the experimental hydrogen bond energy ($E_{HB,exp}$).

A designed experiment and atoms in molecules (AIM) method were used to confirm the strength of hydrogen bonds.

Stable congeners with substitutional HOs at different positions can be ascertained from the analysis of hydrogen bond. The $\log K_{ow}$ of DF and 135 stable PHODF congeners were calculated on-line with molinspiration methodology, which was based on group contributions [28].

The multiple linear regression method of the Statistical Product and Service Solutions (SPSS) 12.0 for Windows program, which is developed by SPSS Inc. of the USA and widely used in various fields [29], is used to obtain the relationship of S° , $\Delta_f H^\circ$, $\Delta_f G^\circ$ and $\log K_{ow}$ with N_{PHOS} .

The total free energy in water (G_{water}°) was calculated according to the results of a continuum solvation model based on the quantum mechanical charge density of a solute molecule interacting with a continuum description of the solvent (SMD) [30] of Self-consistent Reaction Field Theory (SCRf) on 6-311G** level and ΔG_{water}° of reaction (6) was obtained. The pK_a was then calculated according to Eq. (7) [31].



$$\Delta G_{water}^\circ = G_{water}^\circ(A^-) + G_{water}^\circ(H_2O) - G_{water}^\circ(HA) - G_{water}^\circ(OH^-) \quad (6)$$

$$pK_a(HA) = \frac{\Delta G_{water}^\circ}{2.303RT} + 15.74 \quad (7)$$

The most likely ionization paths of di-HODFs were analyzed and the smallest pK_{a1} s of all PHODFs were revealed.

A neutralization reaction experiment with pyrocatechol and hydroquinone as examples was performed, and that intramolecular hydrogen bond energy could be calculated by comparison of $\Delta_f G^\circ$ between isomers was verified [32]. The schematic diagram for determining the experimental hydrogen bond energy ($E_{HB,exp}$) is shown in Fig. 4, and the following reaction steps were adopted. 0.4404 g (0.004 mol) of each tested chemical was dissolved in 40.00 mL of acetonitrile, with the existence of intramolecular hydrogen bond in pyrocatechol and the elimination in hydroquinone. The Apresys 179A-T1 high-precision temperature recorder was inserted into the mixture with the stirring speed of about 420 r min^{-1} . All the reaction occurs in a 100 mL of adiabatic reactor. 3.60 mL of NaOH aqueous solution with concentration of 5.00 mol L^{-1} was added to prompt neutralization reaction, generating hydrated ions. The control experiment, i.e., adding the NaOH solution to pure acetonitrile was also carried out. The reason why we choose acetonitrile as solvent is that: (1) there is no intermolecular hydrogen bond between it and the solute molecule, (2) it is miscible with water, favorable to the conduction of the reaction,

and (3) the temperature of the system increases for the pure neutralization reaction while it slightly declines when water is added in the blank experiment. The overall result is that the heat exchange between the system and the environment is reduced and thus the measurement accuracy of the experiment was improved. The measured heat of reaction was denoted by ΔH_o and ΔH_p . The formula for calculating the reaction heat $\Delta H_{o(p)}$ is:

$$\Delta H_{o(p)} = - \frac{\sum_{i=1}^m (C_{p,i} \times n_i) \times \Delta t}{n} \quad (8)$$

where $C_{p,i}$ is the heat capacity at constant pressure for acetonitrile and water, is 21.860 cal K⁻¹ mol⁻¹ and 17.995 cal K⁻¹ mol⁻¹ [33], respectively, n_i is the moles of acetonitrile and water in the reaction system, n is the moles of test chemical added, Δt is the actual temperature change caused by the neutralization reaction, i.e., the difference between the temperature change of the sample experiment and that of the control test.

ΔH_{ion} is the difference of energies for ions generated from the neutralization reaction. The ions tend to be combined with water molecule to form hydrated ions. Our previous experiment confirmed that four water molecules were most suitable for the calculation, as more water molecules only strengthen the interaction among water molecules.

The intramolecular hydrogen bond energy $E_{HB,exp}$ is available according to Eq. (9):

$$E_{HB,exp} = \Delta H_o - \Delta H_p + \Delta H_{ion} \quad (9)$$

3. Results and discussion

3.1. The influence of the orientation of the hydroxyl on stability

The temperature change of pyrocatechol and hydroquinone turns out to be -3.88°C and -3.20°C respectively. The corresponding value for the control experiment is -4.40°C . Thus, the Δt is respectively 0.52°C and 1.20°C . Thus the ΔH_o and ΔH_p are $-11.216 \text{ kJ mol}^{-1}$ and $-25.883 \text{ kJ mol}^{-1}$ respectively according to Eq. (8). The ΔH_{ion} calculated is $-1.240 \text{ kJ mol}^{-1}$ with MPWB1K/6-311+G(3df,2p)//MPWB1K/6-31+G(d,p) method [34], which is more accurate than the B3LYP/6-311G**. So $E_{HB,exp}$ is $13.427 \text{ kJ mol}^{-1}$ according to Eq. (9). In addition, E° difference between pyrocatechol and hydroquinone at standard state calculated on the MPWB1K/6-311+G(3df,2p)//MPWB1K/6-31+G(d,p) level is $11.764 \text{ kJ mol}^{-1}$, H° difference between them is $10.720 \text{ kJ mol}^{-1}$, and the G° difference is $11.983 \text{ kJ mol}^{-1}$. It is found that the difference among E° , H° and G° is negligible, and the experimental and calculated values are parallel. According to the designed isodesmic reaction, G° difference and $\Delta_f G^\circ$ difference between two molecules are equal. So the energy of hydrogen bond was obtained by comparing $\Delta_f G^\circ$ s between two isomers, which facilitates analyzing the stability of congeners.

As previously mentioned, intramolecular hydrogen bond will affect the molecular energy greatly. In this study, $\Delta_f G^\circ$ s of isomers with hydroxyls replaced in the monoring were calculated based on isodesmic reactions and then compared. There are three kinds of intramolecular hydrogen bonds in monoring-replaced PHODFs. The hydrogen bond between oxygen atom in the matrix and the hydrogen atom of a hydroxyl is defined as the first type of hydrogen bond (Type I), the one between two ortho-position hydroxyls as the second type of hydrogen bond (Type II), and the one between the oxygen atom of hydroxyl at position 1 and the hydrogen atom at position 9 of the matrix as the third type of hydrogen bond (Type III). All the monoring-replaced congeners, with the number of hydrogen bonds and the corresponding $\Delta_f G^\circ$ are listed in Table 1.

As Table 1 shows, 4-mono-HODF has the hydrogen bond (Type I), which does not exist in 4'-mono-HODF, so the $\Delta_f G^\circ$ of 4-mono-HODF is $8.394 \text{ kJ mol}^{-1}$ smaller than that of 4'-mono-HODF.

Similarly, the $\Delta_f G^\circ$ of 2,4-di-HODF is $10.570 \text{ kJ mol}^{-1}$ smaller than that of 2,4'-di-HODF, the $\Delta_f G^\circ$ of 1,4-di-HODF is $8.997 \text{ kJ mol}^{-1}$ smaller than that of 1,4'-di-HODF, and so is 2',4-di-HODF compared to 2',4'-di-HODF. The energy of hydrogen bond of Type I is approximately $8\text{--}11 \text{ kJ mol}^{-1}$. From Table 1 we can also see that the $\Delta_f G^\circ$ of 3'-mono-HODF ($-350.234 \text{ kJ mol}^{-1}$) is almost equal to that of 3-mono-HODF ($-350.052 \text{ kJ mol}^{-1}$). The reason may be the hydroxyl substituted at position 3 is too far away from oxygen in the matrix to form a hydrogen bond (Type I). So do the congeners with a hydroxyl substituted at position 2.

Approximately a $16\text{--}21 \text{ kJ mol}^{-1}$ difference of $\Delta_f G^\circ$ is brought by hydrogen bond of Type II. For instance, $\Delta_f G^\circ$ of 3,4-di-HODF is $16.063 \text{ kJ mol}^{-1}$ smaller than that of 3',4-di-HODF, and 2',3'-di-HODF is $20.028 \text{ kJ mol}^{-1}$ smaller than that of 2',3-di-HODF, respectively.

The most stable isomer with a hydroxyl located at position 1 is 1-mono-HODF, not 1'-mono-HODF, different from the case that a hydroxyl substituted position 2 or 3. The reason is that in the 1-mono-HODF the oxygen of hydroxyl forms a hydrogen bond (Type III) with the hydrogen atom at position 9. Comparing 1-mono-HODF and 2-mono-HODF, the energy of the Type III hydrogen bond is approximately 7.9 kJ mol^{-1} . And $\Delta_f G^\circ$ of 2,3-di-HODF ($-503.255 \text{ kJ mol}^{-1}$) is $5.372 \text{ kJ mol}^{-1}$ bigger than 1,2-di-HODF ($-508.597 \text{ kJ mol}^{-1}$). The energy of hydrogen bond (Type III) is approximately $5\text{--}8 \text{ kJ mol}^{-1}$.

Table 1 also lists the possible conformational isomers that 3 or 4 hydroxyls replaced in one benzene ring, the number of three types of hydrogen bonds and their $\Delta_f G^\circ$. The same conclusions can be obtained by comparing the $\Delta_f G^\circ$ values.

Then we studied the entrance geometry on main paths by atoms in molecules (AIM) method. According to the topological analysis theory put forward by Bader [35,36], the value of electron density $\nabla\rho(r)$ is used to describe the strength of a bond and Laplacian of the electron density $\nabla^2\rho(r)$ to describe the characteristic of the bond. A bigger $\nabla\rho(r)$ indicates stronger bond energy. $\nabla^2\rho(r) < 0$ means that the bond is covalent and the covalency is stronger when $\nabla^2\rho(r)$ is smaller. Conversely $\nabla^2\rho(r) > 0$ means that the bond is ionic and the ionicity is stronger when $\nabla^2\rho(r)$ is bigger. The molecular graph is intuitionistic for the topological property of electron density, and can display the structure of bond systematically. In the molecular graphs, the bond critical point (BCP) represented by the red one indicates that it holds a bond action between the corresponding atoms. There are three criteria for the existence of hydrogen bond within the AIM formalism according to Popelier [37]: (1) bond paths and BCP exist between the interacting atoms; (2) the $\nabla\rho(r)$ value at the BCP is within the range of $0.002\text{--}0.034 \text{ a.u.}$; (3) the $\nabla^2\rho(r)$ value at the BCP is within the range of $0.024\text{--}0.139 \text{ a.u.}$

The entrance geometry on main paths by AIM is shown in Fig. 5. In 1-mono-HODF, a BCP exists between the oxygen atom of hydroxyl at position 1 and the hydrogen atom at position 9. The $\nabla\rho(r)$ is 0.005 a.u. and $\nabla^2\rho(r)$ is 0.021 a.u. The $\nabla^2\rho(r)$ value is lower than the lower limit value of 0.024 a.u. proposed by Popelier, suggesting that the hydrogen bond formed (Type III) is less ionic than conventional hydrogen bond. In 2',3'-di-HODF, a BCP exists between two *ortho* hydroxyls and a hydrogen bond of Type II forms. The $\nabla\rho(r)$ is 0.020 a.u. and $\nabla^2\rho(r)$ is 0.092 a.u. , satisfying the qualifications by Popelier. We also find that a BCP point exists in 1,9'-di-HODF, with the $\nabla\rho(r)$ of 0.028 and $\nabla^2\rho(r)$ of 0.107 , which also satisfy the qualifications of hydrogen bond. It is a little stronger than that of hydrogen bond (Type II), and is defined as the fourth type of hydrogen bond (Type IV). $\Delta_f G^\circ$ of 1,9'-di-HODF is $24.853 \text{ kJ mol}^{-1}$ smaller than that of 2',7'-di-HODF and $23.422 \text{ kJ mol}^{-1}$ smaller than that of 3',7'-di-HODF. The energy of this type of hydrogen bond is approximately $23\text{--}25 \text{ kJ mol}^{-1}$.

According to the thermodynamic principle, a congener possessing smaller $\Delta_f G^\circ$ is more stable than the one possessing larger $\Delta_f G^\circ$,

Table 1
The monoring-replaced congeners, with their number of hydrogen bonds and the $\Delta_f G^\circ$ values.

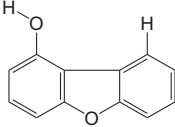
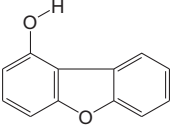
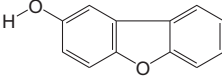
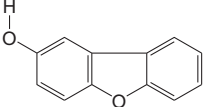
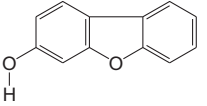
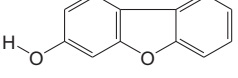
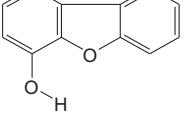
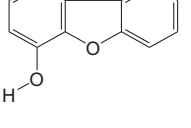
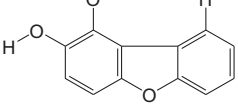
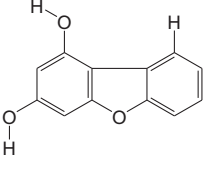
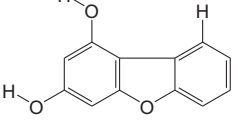
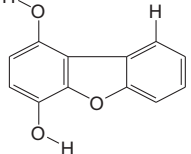
Molecule	Configuration	Type of hydrogen bonds			$\Delta_f G^\circ$ (kJ mol ⁻¹)
		I	II	III	
1-Mono-HODF		0	0	1	−353.809
1'-Mono-HODF		0	0	0	−352.912
2-Mono-HODF		0	0	0	−345.904
2'-Mono-HODF		0	0	0	−346.077
3-Mono-HODF		0	0	0	−350.052
3'-Mono-HODF		0	0	0	−350.234
4-Mono-HODF		1	0	0	−346.553
4'-Mono-HODF		0	0	0	−338.159
1,2-Di-HODF		0	1	1	−508.597
1,3-Di-HODF		0	0	1	−509.572
1,3'-Di-HODF		0	0	1	−507.153
1,4-Di-HODF		1	0	1	−498.460

Table 1 (Continued)

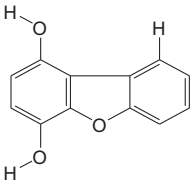
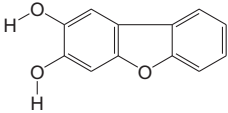
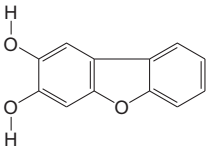
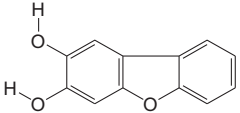
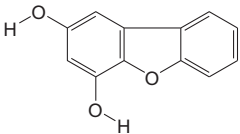
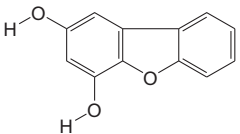
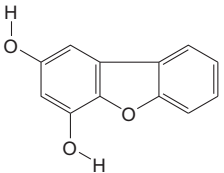
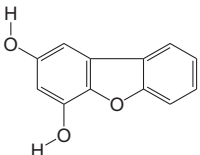
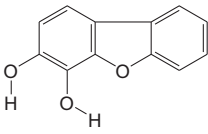
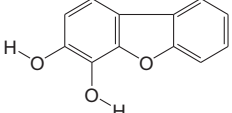
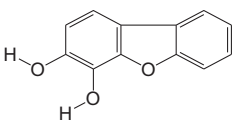
Molecule	Configuration	Type of hydrogen bonds			$\Delta_r G^\circ$ (kJ mol ⁻¹)
		I	II	III	
1,4'-Di-HODF		0	0	1	-489.463
2,3-Di-HODF		0	1	0	-503.255
2',3-Di-HODF		0	0	0	-485.385
2',3'-Di-HODF		0	1	0	-505.413
2,4-Di-HODF		1	0	0	-498.405
2,4'-Di-HODF		0	0	0	-487.835
2',4-Di-HODF		1	0	0	-498.363
2',4'-Di-HODF		0	0	0	-490.608
3,4-Di-HODF		1	1	0	-501.721
3',4-Di-HODF		1	0	0	-485.659
3',4'-Di-HODF		0	1	0	-494.441

Table 1 (Continued)

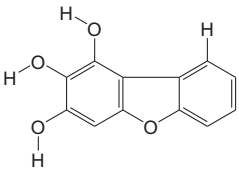
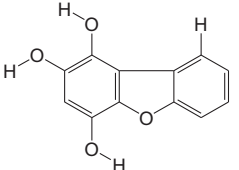
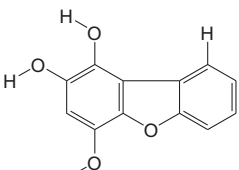
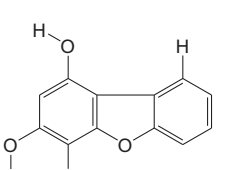
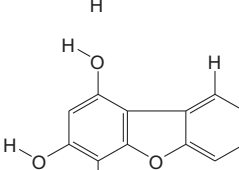
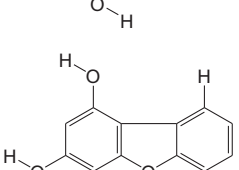
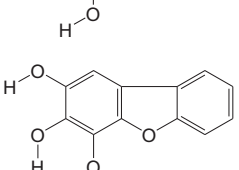
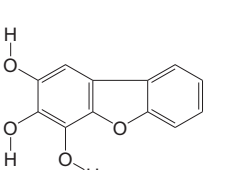
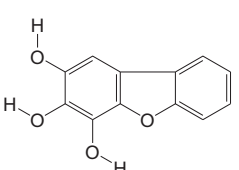
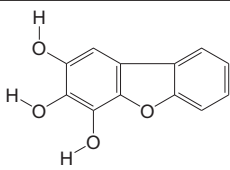
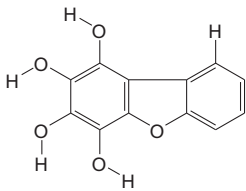
Molecule	Configuration	Type of hydrogen bonds			$\Delta_f G^\circ$ (kJ mol ⁻¹)
		I	II	III	
1,2,3-Tri-HODF		0	2	1	−663.428
1,2,4-Tri-HODF		1	1	1	−652.786
1,2,4'-Tri-HODF		0	1	1	−639.698
1,3,4-Tri-HODF		1	1	1	−655.748
1,3',4-Tri-HODF		1	0	1	−636.311
1,3',4'-Tri-HODF		0	1	1	−644.534
2,3,4-Tri-HODF		1	2	0	−655.417
2',3,4-Tri-HODF		1	1	0	−638.013
2',3',4-Tri-HODF		1	1	0	−641.638

Table 1 (Continued)

Molecule	Configuration	Type of hydrogen bonds			$\Delta_f G^\circ$ (kJ mol ⁻¹)
		I	II	III	
2',3',4'-Tri-HODF		0	2	0	-649.476
1,2,3,4-Tetra-HODF		1	3	1	-809.869

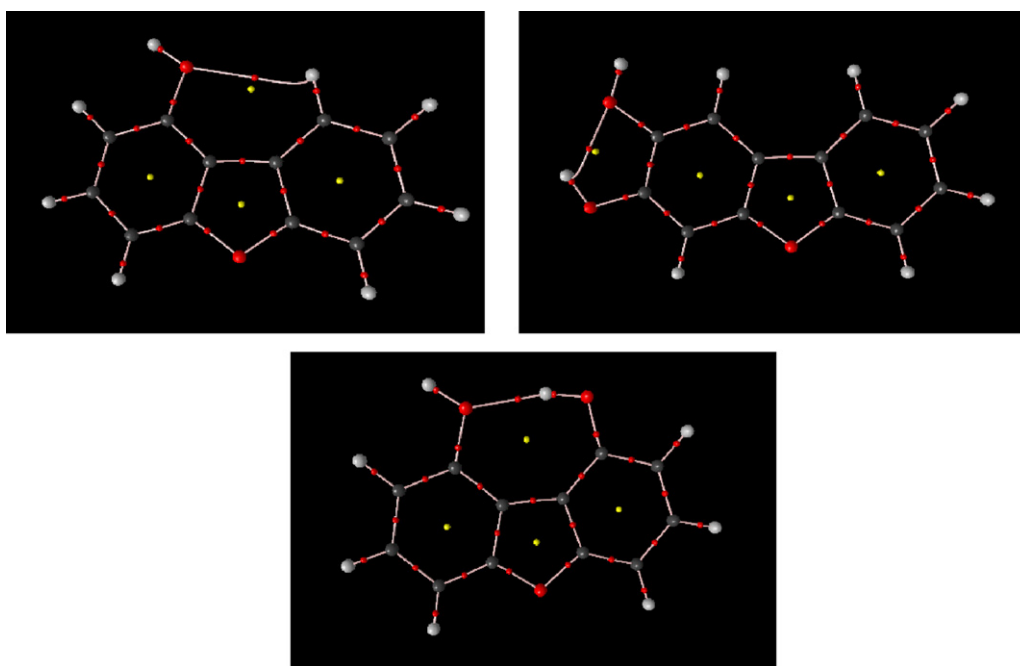


Fig. 5. Analysis of the AIM in 1-mono-HODF, 2',3'-di-HODF and 1,9'-di-HODF (the yellow point indicates that a ring structure exists, the red point indicates that it holds a bond action between the corresponding atoms).

and the stable one forms more easily. We can see that the hydrogen bond influences the stability of congeners. The 135 stable congeners are listed in Table 2. They are determined according to the following principles: the molecules possess hydrogen bonds as much as possible and give priority to the hydrogen bond of Type IV, followed by hydrogen bond of Type II, and then the hydrogen bond of Types I and III. When two benzene rings are both substituted with hydroxyls, conformers with each oxygen atom composing only one hydrogen bond are more stable. The thermodynamic properties, $\log K_{ow}$ s and pK_{a1} s of them are also listed in Table 2.

3.2. Relations of thermodynamic properties and N_{PHOS}

$\Delta_f H^\circ$ and $\Delta_f G^\circ$ of PHODFs were obtained by designing isodesmic reactions. We have used the multiple linear regression method of the SPSS 12.0 for Windows program to obtain the relationship between thermodynamic properties and N_{PHOS} , and the results

are presented in Table 3. Eqs. (10)–(12) show good relationships between S° , $\Delta_f H^\circ$, $\Delta_f G^\circ$ and N_{PHOS} , with R^2 s that are greater than 0.98. Following conclusions can be obtained:

- Substitute number is the main factor influencing the thermodynamic parameters. The value of S° increases with the substitute number of hydroxyls, and $\Delta_f H^\circ$ and $\Delta_f G^\circ$ act the opposite. The influence of N_1 is bigger than others. When N_1 adds one, S° increases by 28.502 J mol⁻¹·K⁻¹, and $\Delta_f H^\circ$ and $\Delta_f G^\circ$ decrease by 182.509 kJ mol⁻¹ and 161.083 kJ mol⁻¹, respectively.
- The relative position for these hydroxide radical (N_o , N_m , N_p) also has small effects on such values. N_m is the main factor influencing S° and N_p influences $\Delta_f H^\circ$ and $\Delta_f G^\circ$ maximally.
- $N_{1,9}$ decreases S° , $\Delta_f H^\circ$ and $\Delta_f G^\circ$. The hydrogen bond of Type IV makes the molecule more stable.
- The squared correlation coefficients R^2 are all bigger than 0.98 for the three properties. Thus they can be predicted from N_{PHOS}

Table 2The stable congeners of PHODF, with their thermodynamic properties, $\log K_{ow}$ s and pK_{a1} s.

Symbolic number	Molecule	Group	S° (J mol ⁻¹ K ⁻¹)	$\Delta_f H^\circ$ (kJ mol ⁻¹)	$\Delta_f G^\circ$ (kJ mol ⁻¹)	$\Delta_f G^\circ_R$ (kJ mol ⁻¹)	$\log K_{ow}$	pK_{a1}
1	DF	C _{2v}	378.693	47.300	142.480	–	3.570	–
	Mono-HODF							
2	1–	C _s	408.439	–483.806	–369.029	0.000	3.303	7.547
3	2'–	C _s	409.723	–475.665	–361.268	7.761	3.067	11.123
4	3'–	C _s	409.113	–479.895	–365.317	3.712	3.067	8.644
5	4–	C _s	408.795	–476.413	–361.741	7.290	3.303	8.551
	Di-HODF							
6	1,2–	C _s	438.495	–658.567	–522.825	18.557	2.807	8.144
7	1,3–	C _s	432.461	–662.479	–524.939	16.444	2.776	7.010
8	1,4–	C _s	435.129	–651.029	–514.284	27.098	3.036	8.652
9	1,6–	C _s	433.080	–657.488	–520.131	21.251	3.036	7.113
10	1,7'–	C _s	433.682	–661.410	–524.232	17.150	2.800	8.222
11	1,8'–	C _s	433.305	–658.491	–521.202	20.180	2.800	7.197
12	1,9'–	C _s	428.697	–680.046	–541.382	0.000	3.036	2.904
13	2',3'–	C _s	436.810	–657.010	–520.764	20.618	2.578	7.156
14	2,4–	C _s	434.142	–650.998	–513.956	27.426	2.776	7.736
15	2',6–	C _s	434.100	–650.370	–513.318	28.064	2.800	8.433
16	2',7'–	C _s	434.393	–653.497	–516.529	24.853	2.564	9.206
17	2',8'–	C _{2v}	429.036	–648.866	–510.301	31.081	2.564	11.136
18	3,4–	C _s	435.271	–654.180	–517.477	23.905	2.807	6.155
19	3',6–	C _s	433.581	–654.242	–517.033	24.349	2.800	8.551
20	3',7'–	C _{2v}	428.187	–656.776	–517.960	23.422	2.564	9.264
21	4,6–	C _{2v}	429.286	–648.325	–509.839	31.543	3.036	8.034
	Tri-HODF							
22	1,2,3–	C _s	461.011	–838.518	–679.564	17.932	2.515	6.097
23	1,2,4–	C _s	464.741	–826.614	–668.773	28.723	2.515	8.483
24	1,2,6–	C _s	466.632	–832.390	–675.114	22.382	2.539	7.813
25	1,2,7'–	C _s	466.912	–836.573	–679.377	18.119	2.303	8.389
26	1,2,8'–	C _s	466.038	–833.270	–675.815	21.681	2.303	8.096
27	1,2,9'–	C _s	459.184	–855.986	–696.488	1.008	2.539	4.012
28	1,3,4–	C _s	462.216	–830.447	–671.853	25.643	2.515	7.659
29	1,3,6–	C _s	457.528	–835.696	–675.704	21.792	2.508	7.110
30	1,3,7–	C _s	457.737	–839.175	–679.243	18.252	2.272	7.537
31	1,3,8'–	C _s	457.636	–837.397	–677.437	20.059	2.272	6.974
32	1',3,9–	C _s	453.542	–858.677	–697.496	0.000	2.508	3.180
33	1,4,6–	C _s	461.120	–822.195	–663.275	34.221	2.768	9.228
34	1,4,7'–	C _s	459.928	–828.791	–669.516	27.980	2.532	9.170
35	1,4,8'–	C _s	459.326	–826.126	–666.670	30.826	2.532	8.845
36	1,4,9'–	C _s	455.901	–849.023	–688.543	8.953	2.768	3.983
37	1,6,7–	C _s	459.627	–834.845	–675.479	22.017	2.539	6.373
38	1,6,8–	C _s	457.703	–831.805	–671.863	25.633	2.508	7.316
39	1,7',8'–	C _s	460.409	–839.642	–680.509	16.987	2.310	7.320
40	2,3,4–	C _s	460.053	–830.552	–671.312	26.184	2.515	6.035
41	2',3',6–	C _s	461.107	–831.799	–672.871	24.625	2.310	5.849
42	2',3',7'–	C _s	462.893	–833.590	–675.198	22.298	2.074	7.451
43	2',3',8'–	C _s	462.232	–830.229	–671.640	25.856	2.074	7.351
44	2,4,6–	C _s	459.685	–822.980	–663.632	33.864	2.508	7.552
45	2,4,7'–	C _s	458.565	–829.161	–669.477	28.019	2.272	7.905
46	2,4,8'–	C _s	459.593	–824.902	–665.525	31.971	2.272	7.965
47	2',6,7–	C _s	460.317	–828.239	–669.080	28.416	2.303	6.335
48	3,4,6–	C _s	462.420	–825.601	–667.066	30.430	2.539	5.996
49	3,4,7'–	C _s	460.007	–831.125	–671.871	25.625	2.303	6.592

Table 2 (Continued)

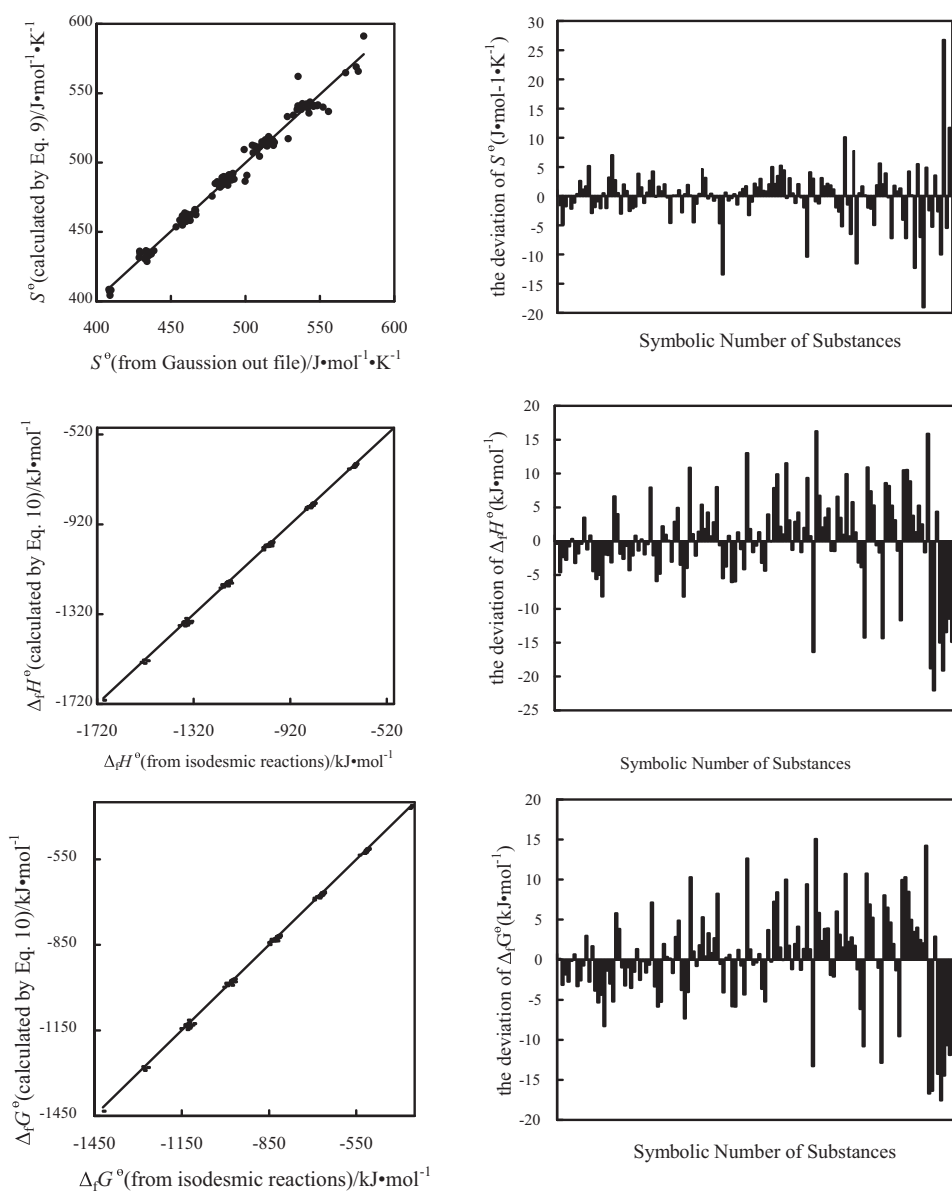
Symbolic number	Molecule	Group	S° (J mol ⁻¹ K ⁻¹)	$\Delta_f H^\circ$ (kJ mol ⁻¹)	$\Delta_f G^\circ$ (kJ mol ⁻¹)	$\Delta_f G^\circ_R$ (kJ mol ⁻¹)	log K_{ow}	pK _{a1}
Tetra-HODF								
50	1,2,3,4-	C _S	487.926	−1007.017	−826.163	26.478	2.453	6.752
51	1,2,3,6-	C _S	486.028	−1011.929	−830.508	22.133	2.248	5.766
52	1,2,3,7'-	C _S	486.509	−1015.489	−834.213	18.428	2.012	6.655
53	1,2,3,8'-	C _S	485.493	−1013.347	−831.768	20.873	2.012	5.590
54	1,2,3,9'-	C _S	479.688	−1034.718	−851.410	1.231	2.248	3.714
55	1,2,4,6-	C _S	491.126	−997.943	−818.042	34.599	2.248	7.906
56	1,2,4,7'-	C _S	490.540	−1004.672	−824.598	28.043	2.012	8.614
57	1,2,4,8'-	C _S	489.307	−1001.595	−821.153	31.488	2.012	8.009
58	1,2,4,9'-	C _S	484.740	−1025.710	−843.906	8.735	2.248	4.373
59	1,2,6,7-	C _S	490.670	−1009.929	−829.894	22.747	2.043	6.356
60	1,2,6,8-	C _S	489.056	−1006.206	−825.690	26.951	2.012	8.084
61	1,2,6,9'-	C _S	486.145	−1020.656	−839.269	13.372	2.272	3.821
62	1,2,7',8'-	C _S	491.636	−1014.641	−834.895	17.746	1.814	7.751
63	1,2,7,9'-	C _S	483.489	−1034.818	−852.641	0.000	2.012	4.666
64	1,2,8,9-	C _{2v}	501.112	−1000.448	−823.527	29.114	2.043	8.533
65	1,3,4,6-	C _S	499.891	−1001.288	−824.002	28.639	2.248	7.233
66	1,3,4,7'-	C _S	488.228	−1007.282	−826.520	26.121	2.012	7.849
67	1,3,4,8'-	C _S	487.521	−1005.699	−824.724	27.917	2.012	7.400
68	1,3,4,9'-	C _S	483.046	−1027.175	−844.867	7.774	2.248	3.532
69	1,3,6,7-	C _S	484.543	−1011.761	−829.899	22.742	2.012	6.285
70	1,3,6,8-	C _S	482.222	−1010.317	−827.762	24.879	1.981	8.134
71	1',3,6,9-	C _S	481.156	−1026.973	−844.103	8.538	2.241	4.371
72	1,3,7',8'-	C _S	485.764	−1017.437	−835.938	16.703	1.783	7.410
73	1,3,7,9'-	C _S	477.731	−1034.850	−850.955	1.686	1.981	3.080
74	1,4,6,7-	C _S	489.010	−999.203	−818.672	33.969	2.272	5.989
75	1,4,6,8-	C _S	485.643	−996.515	−814.981	37.660	2.241	7.692
76	1,4,6,9'-	C _S	483.498	−1010.926	−828.752	23.889	2.501	3.979
77	1,4,7',8'-	C _S	486.065	−1007.358	−825.950	26.691	2.043	7.272
78	1,6,7,8-	C _S	484.405	−1010.858	−828.954	23.687	2.248	6.557
79	2,3,4,6-	C _S	487.425	−1002.091	−821.088	31.553	2.248	5.720
80	2,3,4,7'-	C _S	485.321	−1007.699	−826.068	26.573	2.012	6.033
81	2,3,4,8'-	C _S	485.513	−1004.764	−823.191	29.450	2.012	5.774
82	2',3',6,7-	C _S	486.839	−1008.395	−827.218	25.423	1.814	6.325
83	2',3',6,8-	C _S	486.183	−1006.754	−825.380	27.261	1.783	7.097
84	2',3',7',8- <i>ï</i>	C _{2v}	485.911	−1010.280	−828.825	23.816	1.585	7.424
85	2,4,6,7-	C _S	487.680	−1000.419	−819.491	33.150	2.012	5.843
86	2,4,6,8-	C _{2v}	485.367	−997.289	−815.671	36.970	1.981	7.525
87	3,4,6,7-	C _{2v}	485.702	−1001.726	−820.211	32.430	2.043	6.067
Penta-HODF								
88	1,2,3,4,6-	C _S	516.753	−1177.839	−975.658	30.834	2.186	6.982
89	1,2,3,4,7'-	C _S	513.545	−1184.109	−980.967	25.525	1.950	7.110
90	1,2,3,4,8'-	C _S	513.387	−1182.310	−979.121	27.371	1.950	7.030
91	1,2,3,4,9'-	C _S	507.243	−1204.758	−999.739	6.753	2.186	4.630
92	1,2,3,6,7-	C _S	513.646	−1188.121	−985.010	21.482	1.752	5.165
93	1,2,3,6,8-	C _S	511.065	−1186.046	−982.167	24.325	1.721	5.431
94	1,2,3,6,9'-	C _S	506.357	−1199.032	−993.748	12.744	1.981	3.567
95	1,2,3,7',8'-	C _S	513.834	−1193.692	−990.639	15.853	1.523	6.358
96	1,2,3,7,9'-	C _S	505.181	−1212.125	−1006.492	0.000	1.721	4.758
97	1,2,3,8,9-	C _S	519.467	−1180.551	−979.176	27.316	1.752	5.722
98	1,2,4,6,7-	C _S	518.313	−1175.082	−973.366	33.126	1.752	8.023
99	1,2,4,6,8-	C _S	518.012	−1171.863	−970.055	36.437	1.721	8.205
100	1,2,4,6,9'-	C _S	511.379	−1187.761	−983.973	22.519	1.981	5.358
101	1,2,4,7',8'-	C _S	516.845	−1183.234	−981.080	25.412	1.523	7.127
102	1,2,4,7,9'-	C _S	507.674	−1203.942	−999.051	7.441	1.721	5.920
103	1,2,4,8,9-	C _S	528.747	−1167.862	−969.257	37.235	1.752	7.589

Table 2 (Continued)

Symbolic number	Molecule	Group	S° (J mol ⁻¹ K ⁻¹)	Δ _f H° (kJ mol ⁻¹)	Δ _f G° (kJ mol ⁻¹)	Δ _f G° _R (kJ mol ⁻¹)	log K _{ow}	pK _{a1}
104	1,2,6,7,8-	C _S	515.645	–1185.579	–983.067	23.425	1.752	5.918
105	1,2,6,7,9'-	C _S	514.591	–1200.789	–997.962	8.530	1.752	4.464
106	1,3,4,6,7-	C _S	504.684	–1179.380	–973.594	32.898	1.752	6.384
107	1,3,4,6,8-	C _S	518.857	–1175.781	–974.224	32.267	1.721	7.436
108	1',3,4,6,9-	C _S	499.264	–1192.631	–985.230	21.261	1.981	5.842
109	1,3,4,7',8'-	C _S	514.708	–1185.747	–982.954	23.538	1.523	7.268
110	1',3,4,7,9-	C _S	509.598	–1200.216	–995.898	10.594	1.721	3.504
111	1,3,6,7,8-	C _S	509.585	–1187.997	–983.676	22.816	1.721	6.722
112	1,4,6,7,8-	C _S	514.043	–1175.279	–972.287	34.205	1.981	6.107
113	2,3,4,6,7-	C _S	515.708	–1178.406	–975.910	30.582	1.752	5.957
114	2,3,4,6,8-	C _S	512.554	–1176.621	–973.185	33.307	1.721	5.862
115	2,3,4,7',8'-	C _S	512.763	–1185.261	–981.888	24.604	1.523	6.220
Hexa-HODF								
116	1,2,3,4,6,7-	C _S	548.687	–1353.844	–1131.257	22.976	1.690	6.656
117	1,2,3,4,6,8-	C _S	545.450	–1351.998	–1128.445	25.788	1.659	6.670
118	1,2,3,4,6,9'-	C _S	537.609	–1366.685	–1140.796	13.437	1.919	5.315
119	1,2,3,4,7',8'-	C _S	541.013	–1362.603	–1137.729	16.504	1.461	7.578
120	1,2,3,4,7,9'-	C _S	532.335	–1381.695	–1154.233	0.000	1.659	4.900
121	1,2,3,4,8,9-	C _S	548.177	–1348.493	–1125.754	28.479	1.690	8.037
122	1,2,3,6,7,8-	C _S	538.290	–1364.065	–1138.378	15.855	1.461	5.557
123	1,2,3,6,7,9-	C _S	542.694	–1350.140	–1125.765	28.468	1.461	6.267
124	1,2,3,6,8,9-	C _S	541.803	–1347.490	–1122.850	31.383	1.461	5.437
125	1,2,3,7,8,9-	C _{2V}	534.765	–1359.526	–1132.788	21.445	1.461	6.378
126	1,2,4,6,7,8-	C _S	543.497	–1350.817	–1126.681	27.552	1.461	6.053
127	1,2,4,6,7,9-	C _S	555.813	–1336.406	–1115.945	38.288	1.461	7.510
128	1,2,4,6,8,9-	C _{2V}	545.738	–1332.851	–1109.384	44.849	1.461	8.063
129	1,3,4,6,7,8-	C _S	552.187	–1353.172	–1131.633	22.600	1.461	5.925
130	1,3,4,6,7,9'-	C _S	528.216	–1369.269	–1140.575	13.658	1.461	3.909
131	2,3,4,6,7,8-	C _{2V}	535.392	–1354.781	–1128.230	26.003	1.461	5.573
Hepta-HODF								
132	1,2,3,4,6,7,8-	C _S	574.394	–1529.639	–1284.793	0.000	1.398	5.969
133	1,2,3,4,6,7,9'-	C _S	535.409	–1538.918	–1282.443	2.350	1.398	4.899
134	1,2,3,4,6,8,9-	C _S	575.836	–1512.891	–1268.475	16.317	1.398	6.994
135	1,2,3,4,7,8,9-	C _S	567.355	–1526.817	–1279.870	4.923	1.398	6.465
Octa-HODF								
136	1,2,3,4,6,7,8,9-	C _{2V}	579.512	–1694.268	–1421.021	–	1.336	7.576

Table 3Correlation of the environment-related properties with the number and the relative position of HO substitution (N_{PHOS}).

Eqs.	Descriptor	Constant	N_1	N_2	N_3	N_4	N_o	N_m	N_p	$N_{1,9}$	R^2	SE
(10)	S°	379.910	28.502	28.067	24.371	27.253	1.589	-2.198	-0.189	-5.462	0.984	4.950
(11)	$\Delta_f H^\circ$	-304.045	-182.509	-173.975	-180.445	-172.744	2.279	0.100	5.065	-4.366	0.999	6.964
(12)	$\Delta_f G^\circ$	-210.684	-161.083	-152.418	-157.786	-150.945	1.805	0.756	5.122	-2.736	0.999	6.392
(13)	$\log K_{ow}$	3.680	-0.336	-0.592	-0.586	-0.346	0.151	0.089	0.004	-0.013	0.974	0.077

Note: R^2 , squared correlation coefficient; SE, standard error.**Fig. 6.** Plots of the values obtained from the correlations versus the corresponding DFT results or isodesmic reactions.

of PHODFs. The good correlation is just as that on the properties of PCDFs and polybrominated dibenzofurans (PBDFs) with the number and position of halogen substitution [25,38,39]. Fig. 6 shows plots of the values obtained from the correlations versus the corresponding DFT results or isodesmic reactions. A good predictive ability is seen.

3.3. Relative stability of most stable isomers of each group

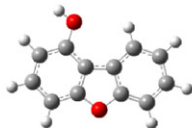
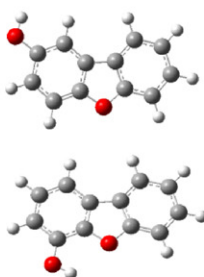
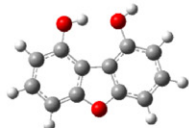
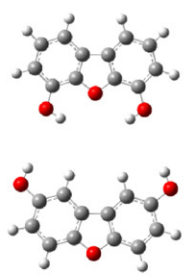
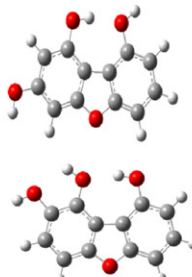
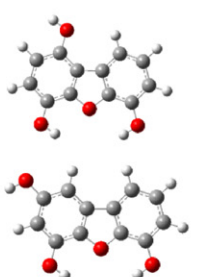
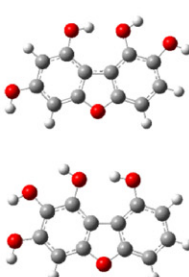
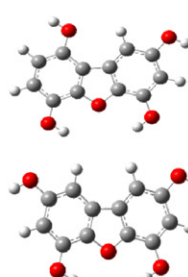
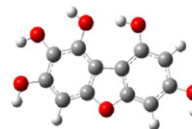
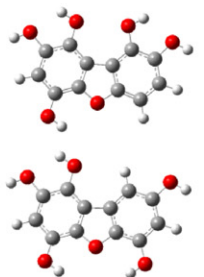
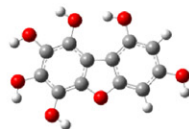
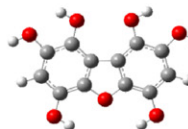
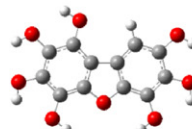
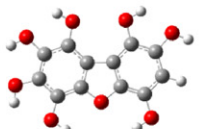
We set the lowest $\Delta_f G^\circ$ in an isomer group to be zero. The relative standard Gibbs energies of formation ($\Delta_f G^\circ_R$) were obtained

by $\Delta_f G^\circ$ of another isomer minus the lowest $\Delta_f G^\circ$. These $\Delta_f G^\circ_R$ values are also listed in Table 2. For each group of isomers, the most and least stable isomers indicated by $\Delta_f G^\circ$ are obtained and listed in Table 4.

As Table 4 shows, in mono-HODFs, 1-mono-HODF is the most stable because of hydrogen bond of Type III. The 4-mono-HODF is less stable owing to the repulsion between oxygen atom of hydroxyl and oxygen in the matrix although there is the hydrogen bond of Type I in it. The most stable isomers of di-HODFs, tri-HODFs, tetra-HODFs, penta-HODFs and hexa-HODFs are always those with hydroxyls substituted position 1 and 9, where a hydrogen bond

Table 4

The most stable and the least stable isomer in different isomer groups for PHODFs.

structure	The most stable molecules	The most unstable molecules	Structure	The most stable molecules	The most unstable molecules
mono-	1- 	2'-; 4- 	di-	1,9'- 	4,6-; 2',8'- 
tri-	1',3,9- ; 1,2,9'- 	1,4,6-; 2,4,6- 	tetra-	1,2,7,9'-; 1,2,3,9'- 	1,4,6,8-; 2,4,6,8- 
penta-	1,2,3,7,9'- 	1,2,4,8,9-; 1,2,4,6,8- 	hexa-	1,2,3,4,7,9'- 	1,2,4,6,8,9- 
hepta-	1,2,3,4,6,7,8- 	1,2,3,4,6,8,9- 			

(Type IV) forms. On the contrary, the least stable isomers are usually those with hydroxyls substituted position 4 and 6, where two hydrogen bonds of Type I form with the same oxygen atom, decreasing the conformation stability notably. It can be interpreted by that there exists repulsion between oxygen atom of the hydroxyl and oxygen of carbonyl in DF and the saturation of hydrogen bond. The key bond lengths and angles of all the structures in Table 4 were put in [supplementary information I](#).

3.4. Octanol-water partition coefficient $\log K_{ow}$

The relationship between $\log K_{ow}$ and N_{PHOS} is presented as Eq. (13) in Table 3. Following regulations were found: the number of HOs- has much more important effect than their position. The $\log K_{ow}$ decreases by 0.592 or 0.586 respectively when N_2 or N_3 adds by one. Comparing to the hydroxyls at position 1,4,6,9, hydroxyls substituted positions 2,3,7,8 decrease $\log K_{ow}$ more notably. But

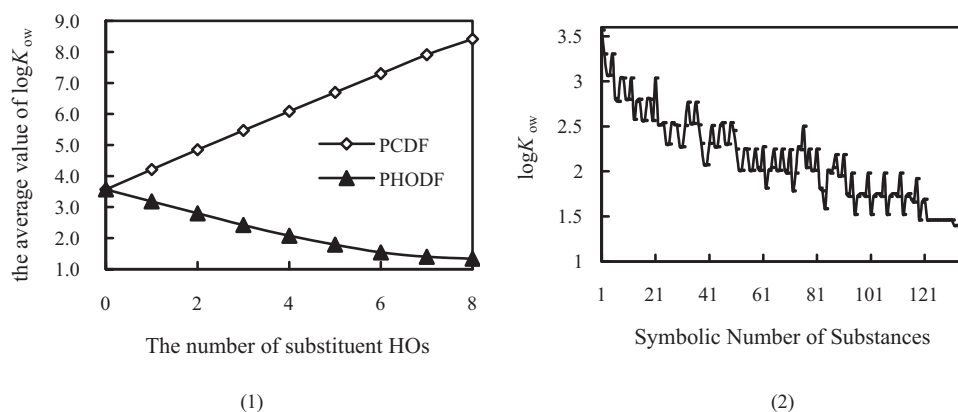


Fig. 7. Relations between log Kow and the number of HOs.

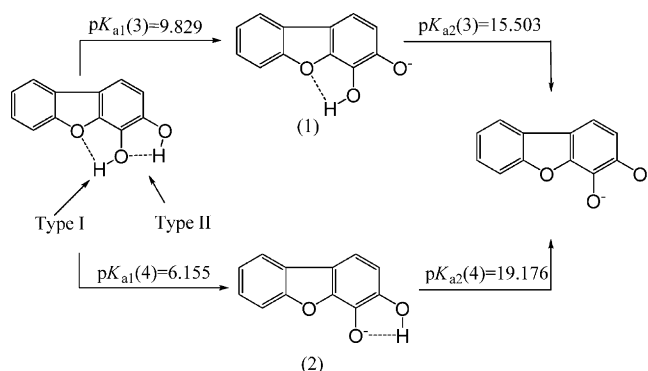


Fig. 8. The possible ionization pathways of 3,4-di-HODF.

when N_o , N_m , N_p add one, the $\log K_{ow}$ only increases by 0.151, 0.089 and 0.004, respectively. When there is only one hydroxyl in the benzene ring, the $\log K_{ow}$ of the conformation with hydroxyl at position 2 or 3 is much smaller than that with hydroxyl at position 1 or 4. What is more, *ortho* substitution will enlarge $\log K_{ow}$ values, and isomers with positions 1,2,3,4 all substituted have larger $\log K_{ow}$ values than its isomers. It indicates that intramolecular hydrogen bonds reinforce hydrophobicity of chemicals slightly.

Fig. 7 shows the trend of $\log K_{ow}$ varying with the number of substituents for PCDFs and PHODFs. We can see clearly that $\log K_{ow}$ decreases with the increasing number of hydroxyl groups in PHODFs, while it increases with the increasing number of the substituent groups in PCDFs. The reason for this may be the hydrophilicity of hydroxyls.

3.5. Ionization of PHODFs

The pK_a s of monoring-replaced PHODFs are calculated and listed in Table 2. The pK_a of 1-mono-HODF is the smallest of all the mono-HODFs, which can be interpreted by that the intramolecular hydrogen bond of Type III facilitates the ionization of hydroxyl.

The pK_{a1} and pK_{a2} values of di-HODFs ionizing along different paths are listed in the supplementary information II. Take 3,4-di-HODF in which two types of hydrogen bonds (Types I and Type II) exist as an example, the ionization may occur by two ways as shown in Fig. 8. When ionization occurs at position 3 firstly, the bond (Type II) was eliminated. And when ionization occurs at position 4 firstly, the bond (Type I) vanishes and bond (Type II) becomes one between hydroxyl and oxygen ion. As the hydrogen bond (Type I) is weaker than hydrogen bond (Type II) and the bond energy between hydroxyl and oxygen ion is stronger, ionization product

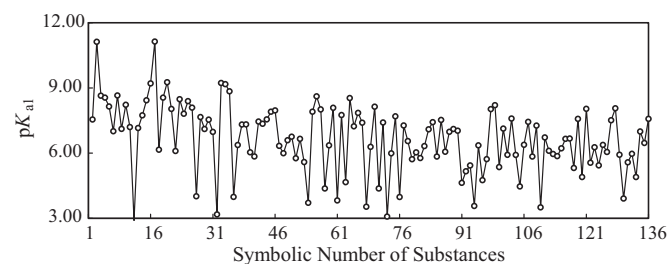


Fig. 9. The relationship between pK_{a1} and the symbolic number of PHODFs.

(2) is more stable than (1). It is obvious that it tends to ionize the hydroxyl at position 4 firstly.

It can be found from the supplementary information II that hydrogen bond (Type I) is always easier to break, theoretically making the ionization intermediate product less stable and the ionization occurs more difficultly. Hydrogen bond (Type III) is always strengthened, making the ionization intermediate product more stable and the ionization occurs more easily. Other two types of hydrogen bond (Types II and IV) may strengthen or restrain the ionization. But two interesting phenomenon can be paid attention to: the hydroxyl at position 2 (8) is always difficult to ionize and the influence of hydrogen bond (Type I) on ionization is small. For example, the hydroxyl at position 2 in 1,2-di-HODF tends to ionize firstly theoretically but in fact the one at position 1 ionizes firstly. The cases of 2,4-, 2',6-, 2',7'- and 3',6-di-HODFs also confirm this. The reason may be that the hydroxyl changes the conjugated system of DF, making the ionization difficult. Hydrogen bond (Type IV) influences the ionization to the greatest degree because the difference of pK_{a1} s between two ionization positions is the greatest about 1,9'-di-HODF. The bond promotes ionization of hydroxyl at position 1 but restrains ionization of hydroxyl at position 9.

In a word, hydrogen bonds of Types II and IV promote ionization of a hydroxyl but restrain ionization of the other hydroxyl, and Type IV has a deeper influence. Hydrogen bond (Type III) promotes ionization of the hydroxyl. The influence of hydrogen bond (Type I) is small. These findings indicate the most likely path of ionization for each congener. Their pK_{a1} s were all calculated (listed in Table 2). The variation trend of pK_{a1} with the symbolic number of PHODFs is presented in Fig. 9. We can see that the pK_{a1} values generally decrease with the number of the hydroxyls, i.e., the first-order ionization of the congener possessing more hydroxyls is easier to occur. The ionization property plays an important part on the migration, transformation and distribution of compounds in the environment. Obviously, an isomer with less substituents is easier to migrate in aqueous solution normally.

4. Conclusions

There are four types of intramolecular hydrogen bonds in PHODFs, and their energies are probably 8–11 kJ mol⁻¹, 16–21 kJ mol⁻¹, 5–8 kJ mol⁻¹ and 23–25 kJ mol⁻¹, respectively. They are obtained by the comparison of $\Delta_f G^\circ$ between isomers. An experiment was designed to approve the validity of this method, and study by AIM also proves the relative magnitude of bond energy. On the basis of analyzing the influence of spatial orientation on molecular stability, 135 stable PHODF congeners with hydroxyls substituted at different positions were ascertained. They were fully optimized to obtain the thermodynamic properties (S° , H° and G°), and their $\log K_{ow}$ s were calculated based on group contributions. The $\Delta_f H^\circ$ and $\Delta_f G^\circ$ of each PHODF congener were calculated by designing isodesmic reactions. Good relations exist between S° , $\Delta_f H^\circ$, $\Delta_f G^\circ$, $\log K_{ow}$ and N_{PHOS} . Substitute number is always the main factor influencing these properties. According to the relative magnitude of their $\Delta_f G^\circ$, the most stable isomers are those with hydroxyls substituted positions 1 and 9, where a hydrogen bond (Type IV) forms. And the least stable isomers are those with two hydrogen bonds of Type I formed with the same oxygen atom. It is also found that the hydrogen bond of Type IV promotes or restrains ionization of hydroxyl in a deeper degree than Type II. Hydrogen bond of Type III usually promotes ionization of the hydroxyl. The influence of hydrogen bond of Type I is small.

Acknowledgements

This work was financially supported by the National Natural Science Foundation of China (Nos. 41071319, 20977046, 20737001) and the Fundamental Research Funds for the Central Universities of China (1112021101).

Appendix A. Supplementary data

Supplementary data associated with this article can be found, in the online version, at <http://dx.doi.org/10.1016/j.jmgs.2012.05.008>.

References

- [1] S.J. Todd, R.B. Cain, S. Schmidt, Biotransformation of naphthalene and daryl ethers by green microalgae, *Biodegradation* 13 (2002) 229–238.
- [2] Q.Z. Zhang, W.N. Yu, R.X. Zhang, Q. Zhou, R. Gao, W.X. Wang, Quantum chemical and kinetic study on dioxin formation from the 2,4,6-TCP and 2,4-DCP precursors, *Environmental Science and Technology* 44 (2010) 3395–3403.
- [3] F. Xu, W.N. Yu, R. Gao, Q. Zhou, Q.Z. Zhang, W.X. Wang, Dioxin formations from the radical/radical cross-condensation of phenoxy radicals with 2-chlorophenoxy radicals and 2,4,6-trichlorophenoxy radicals, *Environmental Science and Technology* 44 (2010) 6745–6751.
- [4] R. Lohmann, W.A. Ockenden, J. Shears, K.C. Jones, Atmospheric distribution of polychlorinated dibenzo-*p*-dioxins, dibenzofurans (PCDD/Fs), and non-ortho biphenyls (PCBs) along a north-south Atlantic transect, *Environmental Science and Technology* 35 (2001) 4046–4053.
- [5] S.Y. Panshin, R.A. Hites, Atmospheric concentrations of polychlorinated biphenyls in Bloomington, Indiana, *Environmental Science and Technology* 28 (1994) 2008–2013.
- [6] M. Tysklind, I. Faengmark, S. Marklund, A. Lindskog, L. Thaning, C. Rappe, Atmospheric transport and transformation of polychlorinated dibenzo-*p*-dioxins and dibenzofurans, *Environmental Science and Technology* 27 (1993) 2190–2197.
- [7] D. Broman, C. Naef, Y. Zebuehr, Long-term high and low-volume air sampling of polychlorinated dibenzo-*p*-dioxins and dibenzofurans and polycyclic aromatic hydrocarbons along a transect from urban to remote areas on the Swedish Baltic Coast, *Environmental Science and Technology* 25 (1991) 1841–1850.
- [8] M. Altarawneh, E.M. Kennedy, B.Z. Dlugogorski, J.C. Mackie, Computational study of the oxidation and decomposition of dibenzofuran under atmospheric conditions, *Journal of Physical Chemistry A* 112 (2008) 6960–6967.
- [9] M. Gesell, E. Hammer, A. Mikolasch, F. Schauer, Oxidation and ring cleavage of dibenzofuran by the filamentous fungus *paecilomyces lilacinus*, *Archives of Microbiology* 182 (2004) 51–59.
- [10] H. Harms, H. Wilkes, R.M. Wittich, P. Fortnagel, Metabolism of hydroxydibenzofurans, methoxydibenzofurans, acetoxydibenzofurans, and nitrodibenzofurans by *Sphingomonas* sp. strain HH69, *Applied and Environment Microbiology* 61 (1995) 2499–2505.
- [11] A. Greenberg, S.E. Stein, R.L. Brown, Relative thermochemical stabilities and reactivities of benzo[*a*]pyrene and selected isomers, *Science of the Total Environment* 40 (1984) 224–230, 219–221.
- [12] R.M. Smith, A.E. Martell, Critical stability constants, enthalpies and entropies for the formation of metal complexes of aminopolycarboxylic acids and carboxylic acids, *Science of the Total Environment* 64 (1987) 125–147.
- [13] X.M. Sun, T.L. Sun, Q.Z. Zhang, W.X. Wang, Degradation mechanism of PCDDs initiated by OH radical in photo-fenton oxidation technology: quantum chemistry and quantitative structure–activity relationship, *Science of the Total Environment* 402 (2008) 123–129.
- [14] P. Schuster, G. Zundel, C. Sanderof, The Hydrogen Bond, Recent Development in Theory and Experiment, Elsevier Science Publishing Co Inc., New York, 1976.
- [15] M. Jablonski, A. Kaczmarek, A.J. Sadlej, Estimates of the energy of intramolecular hydrogen bonds, *Journal of Physical Chemistry A* 110 (2006) 10890–10898.
- [16] A. Nowroozi, H. Raissi, F. Farzad, The presentation of an approach for estimating the intramolecular hydrogen bond strength in conformational study of β -aminoacrolein, *Journal of Molecular Structure: THEOCHEM* 730 (2005) 161–169.
- [17] J.N. Woodford, Density functional theory and atoms-in-molecules investigation of intramolecular hydrogen bonding in derivatives of malonaldehyde and implications for resonance-assisted hydrogen bonding, *Journal of Physical Chemistry A* 111 (2007) 8519–8530.
- [18] E. Eroglu, H. Türkmen, A DFT-based quantum theoretic QSAR study of aromatic and heterocyclic sulfonamides as carbonic anhydrase inhibitors against isozyme, CA-II, *Journal of Molecular Modeling* 26 (2007) 701–708.
- [19] J.N. Latosińska, Structure-activity study of thiazides by magnetic resonance methods (NQR, NMR, EPR) and DFT calculations, *Journal of Molecular Modeling* 23 (2005) 329–337.
- [20] P. Pannopard, P. Khongpracha, M. Probst, J. Limtrakul, Gas sensing properties of platinum derivatives of single-walled carbon nanotubes: a DFT analysis, *Journal of Molecular Modeling* 28 (2009) 62–69.
- [21] Y. Zhao, R.X. Zhang, H. Wang, M.X. He, X.M. Sun, Q.Z. Zhang, W.X. Wang, M.Y. Ru, Mechanism of atmospheric ozonolysis of sabinene: a DFT study, *Journal of Molecular Structure: THEOCHEM* 942 (2010) 32–37.
- [22] A.R. Cherkasov, M. Jonsson, V. Galkin, A novel approach to the analysis of substituent effects: quantitative description of ionization energies and gas basicity of amines, *Journal of Molecular Modeling* 17 (1999) 28–42.
- [23] P. Maurer, V. Thomas, U. Rivard, R. Iftimie, A computational study of ultrafast acid dissociation and acid-base neutralization reactions. I. The model, *Journal of Chemical Physics* 133 (2010) 044108 (1–11).
- [24] J. Qiu, H. Liu, Z.Y. Wang, L.S. Wang, H.X. Yu, DFT study on the thermodynamic properties of polychlorinated phenoxazines, *Acta Chimica Sinica* 24 (2008) 2659–2668.
- [25] J. Yu, X.C. Zhang, Z.Y. Wang, X.L. Zeng, Study on the thermodynamic properties and stability of a series of polybrominated dibenzofurans by density functional theory, *Acta Chimica Sinica* 64 (2006) 1961–1968.
- [26] D.R. Lide, CRC Handbook of Chemistry and Physics, 77th ed., CRC Press, Boca Raton, FL, 1996.
- [27] R. Sabbah, Thermodynamic study of fluorine and dibenzofuran, *Bulletin de la Societe Chimique de France* 128 (1991) 350.
- [28] <http://www.molinspiration.com/cgi-bin/properties>.
- [29] S.B. Green, N.J. Salkind, T.M. Akey, Using SPSS for Windows: Analyzing and Understanding Data, 2nd ed., Prentice Hall, London, 1996.
- [30] A.V. Marenich, C.J. Cramer, D.G. Truhlar, Universal solvation model based on solute electron density and on a continuum model of the solvent defined by the bulk dielectric constant and atomic surface tensions, *Journal of Physical Chemistry B* 113 (2009) 6378–6396.
- [31] J.R. Pliego Jr., J.M. Riveros, Theoretical calculation of pK_a using the cluster-continuum model, *Journal of Physical Chemistry A* 106 (2002) 7434–7439.
- [32] J.Q. Shi, R.J. Qu, A. Flamm, H.X. Liu, Y. Xu, Z.Y. Wang, Environment-related properties of polyhydroxylated dibenzo-*p*-dioxins, *Science of the Total Environment* 414 (2012) 404–416.
- [33] J.A. Dean, Lange's Handbook of Chemistry, 13th ed., Science Press, McGraw-Hill Book Company, 1985.
- [34] Q.Z. Zhang, S.Q. Li, X.H. Qu, X.Y. Shi, W.X. Wang, A quantum mechanical study on the formation of PCDD/Fs from 2-chlorophenol as precursor, *Environmental Science and Technology* 42 (2008) 7301–7308.
- [35] R.F.W. Bader, *Atom in Molecules—A Quantum Theory*, Oxford University Press, Oxford, 1990.
- [36] R.F.W. Bader, A quantum theory of molecular structure and its applications, *Chemical Reviews* 91 (1991) 893–928.
- [37] P.L.A. Popelier, Characterization of a dihydrogen bond on the basis of the electron density, *Journal of Physical Chemistry A* 102 (1998) 1873–1878.
- [38] G.Y. Yang, Y. Jing, Z.Y. Wang, X.L. Zeng, X.H. Ju, QSPR study on the aqueous solubility ($-\lg S_w$) and *n*-octanol/water partition coefficients ($\lg K_{ow}$) of polychlorinated dibenzo-*p*-dioxins (PCDDs), *QSAR & Combinatorial Science* 26 (2007) 352–357.
- [39] Z.Y. Wang, Z.C. Zhai, L.S. Wang, Prediction of gas phase thermodynamic function of polychlorinated dibenzo-*p*-dioxins using DFT, *Journal of Molecular Structure: THEOCHEM* 725 (2005) 55–62.